Cidea-deficient mice have lean phenotype and are resistant to obesity

Article *in* Nature Genetics · October 2003

DOI: 10.1038/ng1225 · Source: PubMed

9 authors, including:

Zhihong Zhou

4 PUBLICATIONS **440** CITATIONS

SEE PROFILE

Ke Guo

Agency for Science, Technology and Research (…

52 PUBLICATIONS **2,207** CITATIONS

SEE PROFILE

Peng Li

Tsinghua University

103 PUBLICATIONS **10,279** CITATIONS

SEE PROFILE

nature genetics

Cidea-deficient mice have lean phenotype and are resistant to obesity

Zhihong Zhou[1], Shen Yon Toh[1], Zhengming Chen[1], Ke Guo[2], Chee Peng Ng[3], Sathivel Ponniah[4], Sheng-Cai Lin[2], Wanjin Hong[3] & Peng Li[1,5]

The thermogenic activity of brown adipose tissue (BAT), important for adaptive thermogenesis and energy expenditure, is mediated by the mitochondrial uncoupling protein1 (Ucp1) that uncouples ATP generation and dissipates the energy as heat. We show here that Cidea, a protein of unknown function sharing sequence similarity with the N-terminal region of DNA fragmentation factors Dffb and Dffa, is expressed at high levels in BAT. *Cidea*-null mice had higher metabolic rate, lipolysis in BAT and core body temperature when subjected to cold treatment. Notably, *Cidea*-null mice are lean and resistant to diet-induced obesity and diabetes. Furthermore, we provide evidence that the role of Cidea in regulating thermogenesis, lipolysis and obesity may be mediated in part through its direct suppression of Ucp1 activity. Our data thus indicate a role for Cidea in regulating energy balance and adiposity.

Obesity is the result of imbalance between energy intake and expenditure[1,2]. BAT increases energy expenditure through thermogenesis, a process whereby energy is dissipated in the form of heat[2–4]. All differentiated brown adipocytes express Ucp1 (refs. 4,5), which resides in the inner mitochondrial membrane and functions to dissipate the proton electrochemical potential gradient as heat, thereby uncoupling the process of ATP synthesis through oxidative phosphorylation. Mice lacking *Ucp1* underwent a rapid decrease in core body temperature during exposure to cold[6]. Exposure of animals to cold or stimulation by pharmacological agents, such as norepinephrine, results in activation of β-adrenergic receptors, elevation of intracellular cAMP, activation of cAMP-dependent protein kinase A and upregulation of Ucp1 activity in BAT[3,4]. Despite abundant evidence that Ucp1 activity is modulated by nucleotides[5,7], free fatty acid (FFA) and coenzyme Q[8], no protein that directly modulates Ucp1 activity in BAT has been identified to date.

Defective BAT function has been associated with obesity[4,9]. Transgenic mice with less BAT, owing to overexpression of diphtheria toxin in brown adipocytes, were obese with symptoms of hyperglycemia and insulin resistance[10]. In addition, greater uncoupling activity in transgenic mice that ectopically express Ucp1 in white adipose tissue (WAT; ref. 11) or Ucp3 in skeletal muscle[12] results in resistance to diet-induced obesity and diabetes. Mice lacking all three β-adrenergic receptors had reduced metabolic rate owing to the lack of diet-induced thermogenesis and developed obesity when fed a high-fat diet[13]. Despite the strong correlation of BAT with obesity, direct evidence of obesity or anti-obesity effects resulting from BAT-specific genes is scarce. Mice deficient in *Ucp1* had normal body weight, which may be due to compensatory effects by other metabolic processes[14,15].

Cidea is a member of the CIDE family of proteins and shares homology with the N-terminal region of the apoptotic DNA fragmentation factors Dffb (or CAD) and Dffa (or ICAD; ref. 16). The structure of the N-terminal domain of Cideb and the complex of N-terminal domains of Dffb and Dffa suggest that N-terminal domains of CIDE family proteins may serve as interaction interfaces or regulatory domains[17,18]. Overexpression of Cidea induced caspase-independent cell death[16]. We showed previously that Cideb is localized to mitochondria and can form homo- or heterodimers with other CIDE family members[19]. Furthermore, the C-terminal region of Cideb, which shares homology with Cidea and fat-specific protein 27 (Fsp27), is responsible for Cideb-induced cell death, mitochondrial localization and dimerization[19]. To study the physiological function of *Cidea* in BAT, we generated *Cidea*-null mice and showed that they are lean and resistant to diet-induced obesity and diabetes.

RESULTS

Cidea is highly expressed in BAT

Northern-blot analysis using *Cidea* cDNA as a probe showed that *Cidea* was highly expressed in BAT (**Fig. 1a**). The expression profile of Cidea closely resembles that of Ucp1, which is predominantly expressed in BAT. The expression of Fsp27 is more widespread, with high levels in WAT and moderate levels in BAT and skeletal muscle (**Fig. 1a**). Consistent with previous observations[16], we also detected small amounts of *Cidea* mRNA in heart, brain, skeletal muscle, lymph node,

Laboratories of [1]Apoptosis Regulation, [2]Regulatory Biology and [3]Membrane Biology and [4]In Vivo Model Unit, Institute of Molecular and Cell Biology, 30 Medical Dr., Singapore 117609, Singapore. [5]Department of Biology, Hong Kong University of Science & Technology, Clear Water Bay, Kowloon, Hong Kong. Correspondence should be addressed to P.L. (bolipeng@ust.hk).

Published online 10 August 2003; doi:10.1038/ng1225

thymus, appendix and bone marrow (data not shown). Expression of *Cidea* was about 50–100 times higher in BAT than in the heart (data not shown), and *Cidea* mRNA was detected in differentiated brown adipocytes but not in undifferentiated preadipocytes (**Fig. 1b**).

We further investigated the detailed spatial and temporal expression profile of *Cidea* by *in situ* hybridization analysis. We detected *Cidea* expression as early as embryonic day (E) 15 in the interscapular region of the embryo (**Fig. 1c**). Similar regions expressed *Ucp1* (**Fig. 1d**), suggesting that this region corresponds to the developing BAT. We detected continued expression of *Cidea* and *Ucp1* in the interscapular region of E18 embryos (**Fig. 1e,f**) and postnatal 1-week-old mice (**Fig. 1g,h**).

Generation of *Cidea*-null mice

To elucidate the biological role of Cidea *in vivo*, we isolated *Cidea* genomic DNA and generated *Cidea*-null mice by homologous recombination (**Fig. 2a**). The targeting knockout vector was designed to remove part of the first intron and the second exon. Deletion of this region disrupts the reading frame and generates a severely truncated Cidea protein containing only the first eight amino acid residues. Southern-blot analysis confirmed that *Cidea* was disrupted (**Fig. 2b**), and northern-blot analysis showed that there was no *Cidea* mRNA transcript in *Cidea*-null mice (**Fig. 2c**). *Cidea*-null mice appear normal and fertile and produce the expected mendelian ratio of heterozygous and homozygous descendents.

Cidea-null mice had higher levels of mRNA of several BAT markers, including Ucp1 (45% higher), Fsp27 (138% higher), lipoprotein lipase (Lpl, 24% higher) and peroxisome proliferator-activated receptor γ (Pparg, 33% higher; **Fig. 2c**), but protein levels for Ucp1, cytochrome c, COX IV and Actb were similar in BAT of wild-type and *Cidea*-null mice at different ages (**Fig. 2d**). Expression levels of several fat-specific

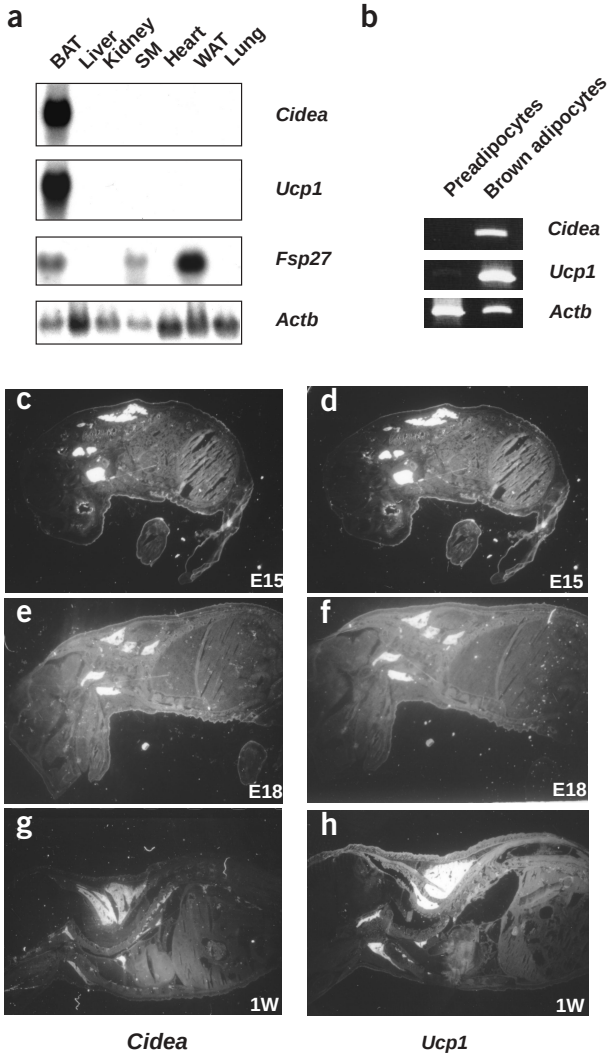

Figure 1 *Cidea* is highly expressed in BAT. (**a**) Northern-blot analysis of RNA isolated from tissues of adult wild-type mice. SM, skeletal muscle. Thirty micrograms of total RNA was loaded in each lane. (**b**) RT–PCR analysis of *Cidea* expression in undifferentiated preadipocytes or differentiated brown adipocytes. (**c**–**h**) *In situ* hybridization analyses of *Cidea* and *Ucp1* in E15 and E18 embryos and in 1-week-old mice (1W).

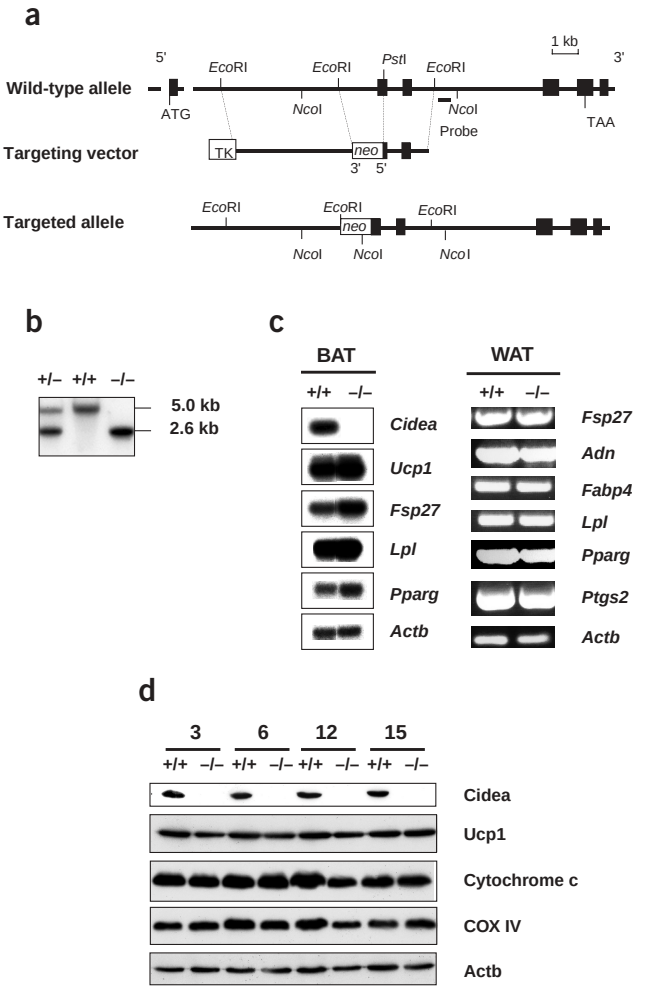

Figure 2 Targeted disruption of *Cidea*. (**a**) Schematic representation of *Cidea* targeted disruption strategy: partial restriction map of the *Cidea* locus (top); gene targeting vector (middle); expected structure of the mutated locus (bottom). The underlined region was used as a probe for Southern-blot analysis. (**b**) Southern-blot analysis of mice with the indicated *Cidea* genotypes. The 5.0-kb and 2.6-kb fragments correspond to the wild-type and mutated alleles, respectively. (**c**) Northern-blot analysis in wild-type (+/+) and *Cidea*-null (–/–) mice (left). *Lpl*, lipoprotein lipase; *Pparg*, peroxisome proliferator-activated receptor-γ. RT–PCR analysis of genes expressed in WAT (right). *Adn*, adipsin; *Fabp4*, fatty acid–binding protein 4. (**d**) Western-blot analysis of Ucp1, COX IV, cytochrome c (total cell lysate) and Cidea (heavy membrane) of BAT isolated from wild-type (+/+) and *Cidea*-null (–/–) mice at 3, 6, 12 and 15 months of age.

markers in WAT were similar between wild-type and *Cidea*-null mice (**Fig. 2c**). These data suggest that BAT and WAT of *Cidea*-null mice had no discernible alterations in development or differentiation. Similarly, the brain, liver and skeletal muscles of *Cidea*-null mice had no obvious morphological defects. The total cell numbers in BAT from wild-type and *Cidea*-null mice before or after cold exposure were also similar (data not shown). In addition, we observed similar percentages of TUNEL-positive cells in sections from BAT of wild-type and *Cidea*-null mice (data not shown). These data suggest that Cidea does not have a direct role in controlling cell death in BAT.

Higher temperature and metabolic rate in *Cidea*-null mice

Because *Cidea* was predominantly expressed in BAT, we assessed the effect of *Cidea* deficiency on thermoregulation and metabolism. When exposed to cold for 1 h, *Cidea*-null male mice had core body temperatures that were 0.6 °C ($P < 0.05$) higher than those of wild-type mice (**Fig. 3a**). Overall, both male and female *Cidea*-null mice had significantly higher core body temperatures than wild-type mice (two-tailed paired *t*-test, $P < 0.01$). We assessed the effect of *Cidea* disruption on whole-body metabolic rates by measuring oxygen consumption and respiratory exchange rate (RER) with indirect calorimetry. Total oxygen consumption rate was 10% higher in *Cidea*-null mice ($P < 0.0001$, **Fig. 3b**) than in wild-type mice. RER, calculated as the ratio of VCO_2 and VO_2, was slightly lower (0.7294 ± 0.003427 versus 0.7207 ± 0.002524; $P < 0.05$; **Fig. 3b**) in *Cidea*-null mice than in wild-type mice, indicating a higher percentage of lipid metabolism in the mutant mice. The increase in body temperature and metabolism in *Cidea*-null mice suggests that Cidea has an important role in regulating energy expenditure.

Enhanced lipolysis in BAT of *Cidea*-null mice

When maintained at room temperature, brown adipocytes of one-month-old wild-type and *Cidea*-null mice contained lipid droplets of similar size (**Fig. 3c,d**), but after overnight exposure to cold, brown adipocytes of *Cidea*-null mice had almost no lipid droplets left (**Fig. 3e,f**). Quantitative analysis of lipid volume density showed that lipid volume in brown adipocytes of wild-type mice exposed to cold (4 °C) overnight decreased from 25% to 12% mice (**Fig. 3i**). Lipid volume density in brown adipocytes of *Cidea*-null mice decreased from 23% to less than 2% (**Fig. 3i**), indicating that *Cidea*-

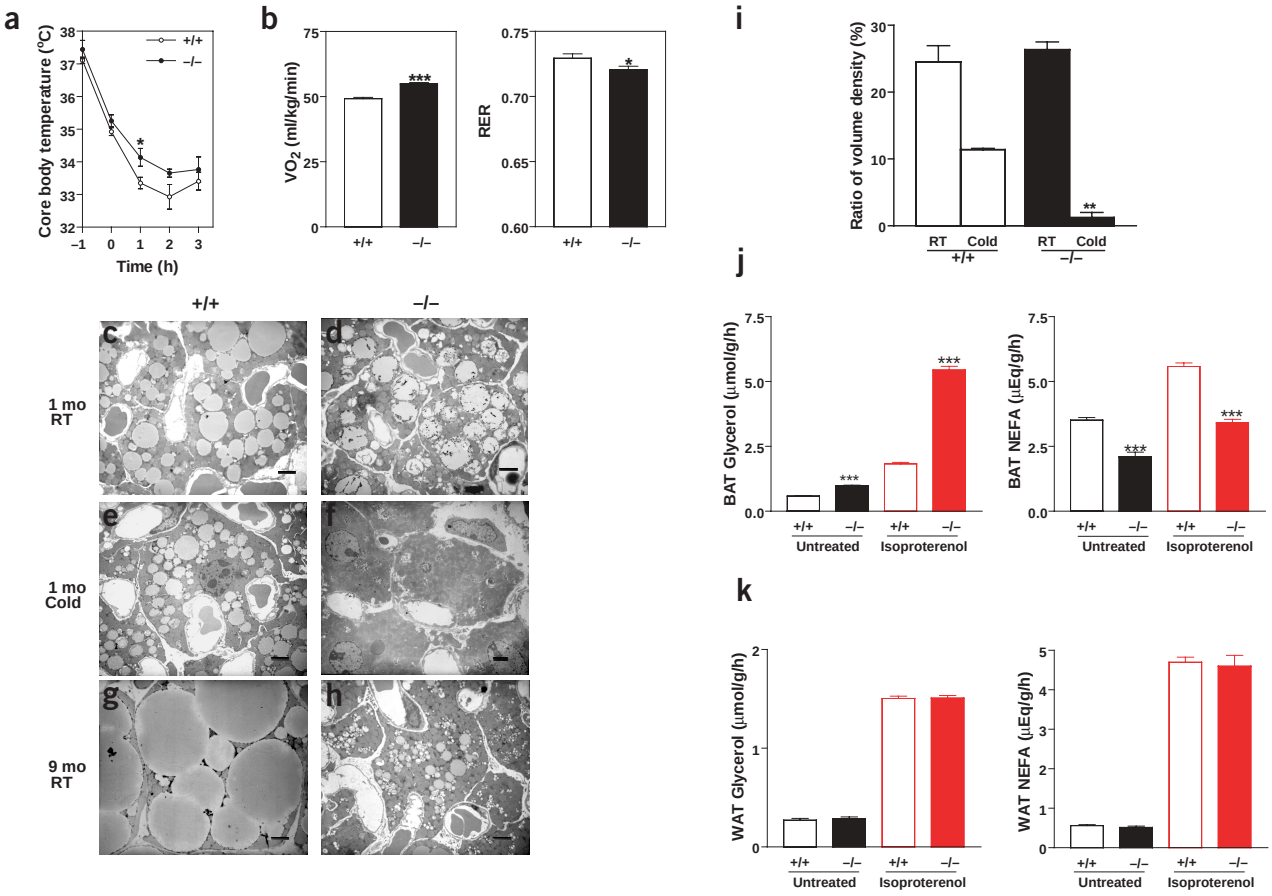

Figure 3 Higher core body temperature, metabolic rate and lipolysis in BAT of *Cidea*-null (–/–) mice relative to wild-type (+/+) mice. (**a**) Core body temperature in 4-week-old wild-type and *Cidea*-null mice of 129 inbred background. Time point –1 was before fasting and before cold exposure; time point 0 was after fasting and before cold exposure. Data shown are mean + s.e.m. of five mice in each group. $^{*}P < 0.05$. (**b**) Whole-body oxygen consumption rate, represented by mean ± s.e.m. of VO_2 for 12 mice in each group (left). Mean ± s.e.m. of RER (VCO_2/VO_2) for 12 fasting mice in each group (right). $^{*}P < 0.05$, $^{***}P < 0.001$. (**c**–**h**) Images of transmission electron microscopy of BAT of wild-type (**c**,**e**,**g**) and *Cidea*-null mice (**d**,**f**,**h**) at 1 month (**c**–**f**) and 9 months (**g**,**h**) of age. Scale bars = 2 μm. RT, room temperature. (**i**) Percentage of lipid volume in BAT of 4-week-old wild-type and *Cidea*-null mice before (room temperature; RT) and after cold exposure. Three male mice were tested in each group. $^{**}P < 0.01$. (**j**,**k**) Greater lipolysis in BAT of *Cidea*-null mice. Seven male mice 5–6 weeks old were used in the test. $^{***}P < 0.001$.

null mice catabolized lipids in BAT at a higher rate. After we removed the mice from the cold and allowed them to recover at room temperature for 1 week, brown adipocytes from wild-type and *Cidea*-null mice had similar amounts of lipid accumulation (data not shown). However, decreased lipid accumulation in brown adipocytes was clearly evident in adult aged *Cidea* null mice as compared with wild-type. Brown adipocytes from nine-month-old wild-type mice contained large lipid droplets that closely resembled those in white adipocytes (**Fig. 3g**), but those from *Cidea*-null mice of the same age contained fewer lipid droplets (**Fig. 3h**). In accordance with the lesser lipid content, the weight of the BAT from nine-month-old *Cidea*-null mice was 60% less than that of the wild-type mice (data not shown). The rapid depletion of lipid and decrease in fat accumulation in BAT were not due to greater lipase activity, as we detected no difference in hormone-sensitive lipase (HSL) activity between BAT from *Cidea*-null and wild-type mice (**Table 1**).

To confirm that lipolysis in BAT is enhanced in *Cidea*-null mice, we determined the amounts of glycerol and FFA released from explants of BAT and WAT that were maintained *in vitro*. The amount of glycerol released from BAT of *Cidea*-null mice was 67% higher than that of wild-type mice (0.5830 ± 0.01580 versus 0.9743 ± 0.03228 μmol g^{-1} h^{-1}) at basal level and 198% higher than that of wild-type mice (1.824 ± 0.05541 versus 5.440 ± 0.1473 μmol g^{-1} h^{-1}) in the presence of isoproterenol (**Fig. 3j**), suggesting enhanced lipolysis. The amount of non-esterified fatty acids (NEFA) released from BAT of *Cidea*-null mice was lower in both basal and isoproterenol-treated tissue relative to that of wild-type mice (**Fig. 3j**). As the complete lipolysis of 1 mol of triacylglycerides yields 1 mol of glycerol and 3 mol of fatty acids, the lower levels of fatty acid released from BAT suggest that *Cidea*-null mice may have increased fatty acid recycling or fatty acid oxidation. On the contrary, no difference in the release of glycerol or NEFA was observed in WAT from wild-type and *Cidea*-null mice (**Fig. 3k**).

Less adiposity and lean phenotype in *Cidea*-null mice

We further examined the roles of Cidea in regulating body weight and adiposity. There was no significant difference in body weight between wild-type and *Cidea*-null mice up to 9 months of age when fed either normal chow or a high-fat diet (**Table 1**). The weight of tissues, including liver, kidney, spleen and heart, was also similar in *Cidea*-null and wild-type mice (**Table 1**). Notably, *Cidea*-null mice had markedly less white adipose tissue. The adiposity index (ratio of total body fat to body weight) was 9.05% and 3.47% ($P < 0.001$) for wild-type and *Cidea*-null male mice, respectively, corresponding to a 62% reduction in *Cidea*-null mice (**Fig. 4a**). We observed a similar reduction in adiposity index in female mice (data not shown). At all ages examined, the adiposity index of heterozygous mice (*Cidea*$^{+/-}$) was intermediate between those of wild-type and *Cidea*-null mice, suggesting that the effect of Cidea on adiposity is gene dose–dependent (data not shown). Lipid content was about 60% lower in *Cidea*-null mice than in wild-type mice, consistent with a lesser lipid accumulation in WAT (**Fig. 4b**). The reduced adiposity was not due to a difference in cell numbers in WAT, as the DNA content (**Fig. 4b**) was similar between wild-type and *Cidea*-null mice. Lesser lipid accumulation in WAT was also not due to enhanced basal HSL activity in WAT, as the activities were similar in *Cidea*-null and wild-type mice (**Table 1**). White adipocytes were also smaller and more compact in the WAT of *Cidea*-null mice relative to wild-type mice (**Fig. 4c,d**).

When fed a high-fat diet (37% of kilocalories from fat) for eight months, wild-type mice became obese, but *Cidea*-null mice had an adiposity index similar to that of wild-type mice fed normal chow. This represents a 36% difference ($P < 0.001$; **Fig. 4a**) in body fat, suggesting that *Cidea*-null mice are protected against obesity induced by a high-fat diet. Consistent with lower amount of WAT, *Cidea*-null mice had 50% less leptin than wild-type mice when fed normal chow (0.99 ± 0.22 versus 2.02 ± 0.2 ng ml^{-1}; $P < 0.01$) and 40% less leptin when fed a high-fat diet (1.96 ± 0.2 versus 3.3 ± 0.16 ng ml^{-1}; $P < 0.01$). The lower levels of leptin in *Cidea*-null mice did not result in hyperphagia, however, because wild-type and *Cidea*-null mice had similar food intakes (**Table 1**). We also observed no difference in physical activity between wild-type and *Cidea*-null mice. Our data thus suggest that Cidea has a direct and important role in regulating adiposity.

Levels of glucose, FFA and triglycerides in *Cidea*-null mice

To evaluate a possible effect of *Cidea* deficiency on the development of diabetes, we tested levels of plasma insulin and glucose. We observed similar levels of insulin and glucose in wild-type and *Cidea*-null mice fed normal chow. Wild-type mice fed a high-fat diet became diabetic with higher blood glucose levels (10.30 ± 0.33 mmol l^{-1}), but plasma glucose levels in *Cidea*-null mice were significantly lower (8.28 ± 0.24 mmol l^{-1}; $P < 0.001$). Furthermore, wild-type and *Cidea*-

Table 1 Metabolic parameters of wild-type and *Cidea*-null mice

Parameter (units)	*n*	Chow			High-fat diet		
		Wild-type	*Cidea*-null	*P* value[a]	Wild-type	*Cidea*-null	*P* value[a]
TG (mmol dl^{-1}) (fed)	8	1.13 ± 0.03	1.14 ± 0.02	$P = 0.66$	ND	ND	
Insulin (ng ml^{-1}) (fed)	8	3.73 ± 0.26	3.62 ± 0.23	$P = 0.76$	5.86 ± 0.28	5.88 ± 0.29	$P = 0.96$
Glucose (mmol l^{-1}) (fed)	8	9.63 ± 0.65	10.12 ± 0.53	$P = 0.58$	10.30 ± 0.33	8.28 ± 0.24	**$P = 0.0002$[b]**
Glucose (mmol l^{-1}) (fast)	8	8.66 ± 0.97	7.64 ± 0.55	$P = 0.36$	8.77 ± 0.48	8.22 ± 0.36	$P = 0.43$
Leptin (ng ml^{-1}) (fed)	8	2.02 ± 0.2	0.99 ± 0.22	**$P = 0.0016$[c]**	3.3 ± 0.16	1.96 ± 0.2	**$P = 0.0004$[b]**
Glycerol (mg ml^{-1}) (fed)	8	16.02 ± 1.19	18.23 ± 0.92	$P = 0.175$	ND	ND	
Glycerol (mg ml^{-1}) (fast)	8	5.59 ± 0.60	4.93 ± 0.98	$P = 0.35$	ND	ND	
WAT HSL activity (mU mg^{-1})	6	2.56 ± 0.8	2.53 ± 0.30	$P = 0.98$	ND	ND	
BAT HSL activity (mU mg^{-1})	6	2.62 ± 0.47	3.86 ± 0.12	$P = 0.061$	ND	ND	
Food intake (g d^{-1})	12	4.05 ± 0.77	4.87 ± 0.68	$P = 0.44$	ND	ND	
Total body weight (g)	8	42.28 ± 2.03	38.27 ± 2.06	$P = 0.21$	49.36 ± 2.39	44.05 ± 1.89	$P = 0.11$
Liver[d]	8	4.31 ± 0.11	4.12± 0.07	$P = 0.23$	4.02 ± 0.18	4.08 ± 0.14	$P = 0.77$
Kidney[d]	8	1.22 ± 0.04	1.44 ± 0.12	$P = 0.12$	1.16 ± 0.06	1.21 ± 0.05	$P = 0.27$
Spleen[d]	8	0.27 ± 0.01	0.29 ± 0.01	$P = 0.40$	0.32 ± 0.05	0.53 ± 0.06	$P = 0.31$
Heart[d]	8	0.51 ± 0.00	0.49 ± 0.00	$P = 0.73$	0.36 ± 0.01	0.40 ± 0.01	$P = 0.16$

[a]*P* values are the results of non-paired Student's *t*-test. [b]$P < 0.001$. [c]$P < 0.01$. [d]Percentage of total body weight. ND, not determined.

null mice were similarly sensitive to exogenously administered insulin (**Fig. 4e**). Notably, *Cidea*-null mice had significantly lower levels of blood glucose after administration of an exogenous load of glucose ($P < 0.001$ by two-tailed paired *t*-test; **Fig. 4f**), suggesting enhanced glucose disposal. These data suggest that Cidea has an important role in regulating insulin sensitivity and glucose disposal.

To further evaluate the rate of lipid metabolism in *Cidea*-null mice, we measured levels of NEFA, triglycerides and glycerol. Wild-type and *Cidea*-null mice had similar levels of triglycerides when fed, but levels of triglycerides and NEFA were about 60% lower ($P < 0.001$) in *Cidea*-null mice than in wild-type mice when fasting (**Fig. 4g,h**), suggesting a higher rate of lipid metabolism in *Cidea*-null mice. Notably, levels of plasma glycerol in both fed and fasted states were similar in wild-type and *Cidea*-null mice (data not shown), suggesting altered fatty acid metabolism in *Cidea*-null mice.

Cidea interacts with and inhibits Ucp1

Cidea-null mice had greater thermogenic and metabolic activity and lipid consumption, suggesting that BAT in *Cidea*-null mice is hyperactive. We reasoned that the greater energy expenditure in BAT could result in less lipid accumulation in WAT and contribute to the lean phenotype of *Cidea*-null mice. To understand the molecular mechanism by which Cidea regulates uncoupling activity, lipolysis and energy expenditure in BAT, we examined the cellular location of Cidea. GFP-Cidea fusion proteins were present in punctate structures overlapping with structures stained by MitoTracker (**Fig. 5a**), indicating that Cidea is localized to the mitochondria. Mitochondrial localization of Cidea was further confirmed by biochemical fractionation. Cidea was present exclusively in a heavy membrane fraction enriched in mitochondria, similar to the localization of Ucp1. Cytochrome c, a mitochondria-specific protein, was also detected exclusively in the same heavy membrane fraction (**Fig. 5b**). As a control, HSL was detected only in cytosolic fractions.

As Cidea and Ucp1 were both localized to mitochondria, we explored the possibility that Cidea interacts with Ucp1 by coexpressing FLAG-tagged Ucp1 with hemagglutinin-tagged Cidea in 293T cells. We immunoprecipitated FLAG-Ucp1 with monoclonal antibodies against the FLAG epitope and detected the coprecipitating proteins with antibodies to hemagglutinin. Hemagglutinin-Cidea coprecipitated with FLAG-Ucp1, indicating a specific interaction between Ucp1 and Cidea (**Fig. 5c**). Immunoprecipitation of FLAG-Cidea also coprecipitated hemagglutinin-Ucp1 (data not shown), confirming this interaction. The interaction between Ucp1 and Cidea did not result merely from colocalization on the mitochondrial membrane, as COX IV and BAX, proteins that localize to mitochondrial inner and outer membrane, respectively, did not coprecipitate with Ucp1. Ucp1Δ3, a truncated form of Ucp1 that lacks three residues in its nucleotide-binding region, resulting in a constitutively active form of Ucp1 (ref. 7), had a similar binding affinity for Cidea to that of full-length Ucp1 (**Fig. 5c**).

To test the functional consequences of the interaction between Cidea and Ucp1, we expressed mouse Ucp1Δ3 and Cidea alone or in combination in yeast under the control of a tightly regulated Gal4 promoter. We used Ucp1Δ3 because wild-type Ucp1 had low uncoupling activity when expressed in yeast. When Ucp1Δ3 was overexpressed in yeast, greater uncoupling activity resulted in lower mitochondrial membrane potential, which we assayed by staining with 3,3′-dihexyloxacarbocyanine iodide (DiOC6). As a control, we added carbonyl cyanide p-(trifluoromethoxy)phenylhydrazone (FCCP), a non-specific chemical uncoupler, before DiOC6 to collapse the membrane potential and abolish DiOC6 accumulation in mitochondria, resulting in a low level of green fluorescence. Yeast cells expressing Ucp1Δ3 had less fluorescence intensity than those transformed with the vector alone (**Fig. 5d**), consistent with greater uncoupling activity and lower mitochondrial membrane potential. Expression of Cidea alone resulted in similar fluorescence intensity to that of the control, suggesting that Cidea itself does not possess uncoupling activity and did not interfere with the yeast metabolic activity. In contrast, expression of both Cidea and Ucp1Δ3 restored the mitochondrial membrane potential (**Fig. 5d**). When yeast cells were cultured in glucose, switching off Cidea and Ucp1Δ3 expression, we observed the same fluorescence intensity for all the yeast transformants (data not shown).

Western-blot analysis of mitochondrial membrane fractions showed that both Cidea and Ucp1Δ3 were associated with yeast mitochondria

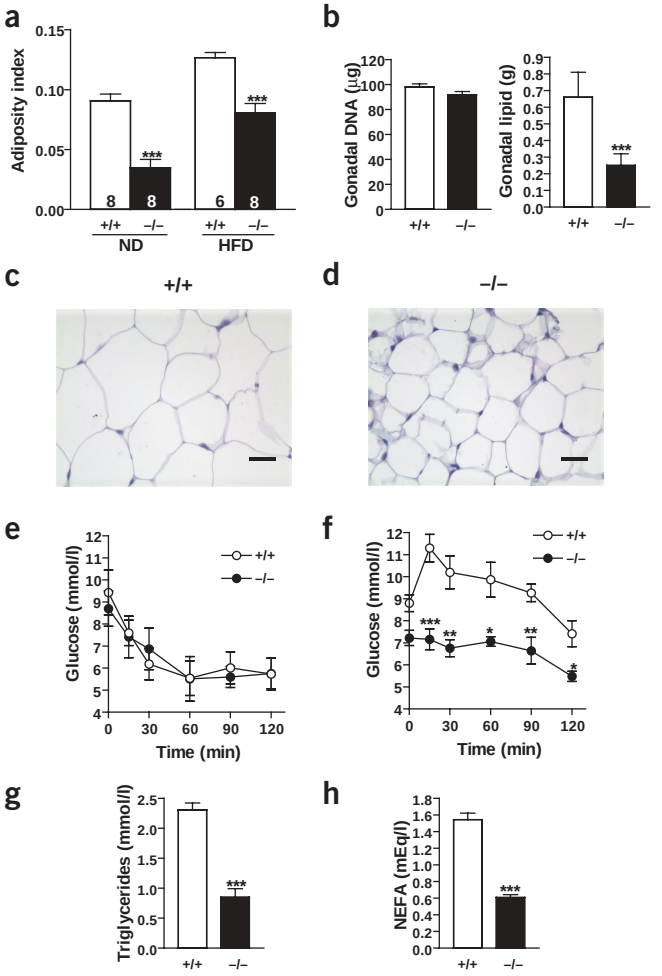

Figure 4 Less adiposity and lean phenotype in *Cidea*-null mice (–/–) compared with wild-type (+/+) mice. (**a**) Adiposity index of mice fed either normal chow (ND) or a high-fat diet (HFD). Number of mice examined in each group is indicated in the respective bars. ***$P < 0.001$. (**b**) Total DNA and lipid contents of gonadal WAT from 9-month-old male mice ($n = 6$) fed normal chow. ***$P < 0.001$. (**c**,**d**) WAT sections stained with hemotoxylin and eosin. Scale bars = 50 μm. (**e**) ITT on 10-week-old wild-type ($n = 7$) and *Cidea*-null ($n = 7$) male mice. (**f**) GTT on 10-week-old wild-type ($n = 7$) and *Cidea*-null ($n = 6$) male mice. *$P < 0.05$, **$P < 0.01$, ***$P < 0.001$. (**g**,**h**) Serum levels of triglycerides and NEFA in 9-month-old wild-type ($n = 8$) and *Cidea*-null ($n = 6$) male mice after fasting overnight. ***$P < 0.001$.

(**Fig. 5e**). Furthermore, overexpression of Cidea and Ucp1Δ3 alone or in combination did not result in mitochondrial proliferation, as levels of mitochondria-specific proteins (COX IVp) in these yeast strains were similar to those in control strains (**Fig. 5e**). Our data thus suggest that Cidea has a role in regulating fat metabolism in BAT by binding to Ucp1 and inhibiting its uncoupling activity. A more direct assessment of enhanced uncoupling activity in *Cidea*-null mice using isolated BAT mitochondria was difficult owing to the large variation among in dividual mice.

DISCUSSION

Adaptive thermogenesis in BAT has been proposed to be a crucial physiological defense mechanism against obesity and diabetes. Although BAT and WAT exert opposite functions in terms of energy expenditure, most genes involved in adipocyte differentiation and lipid metabolism are expressed in both tissues. *Ucp1* is the only gene identified thus far that is expressed specifically in BAT but not in WAT. We showed that *Cidea* is also highly expressed in BAT but not expressed in WAT. *Cidea*-null mice had higher energy expenditure and more active lipid metabolism. Furthermore, BAT of *Cidea*-null mice had enhanced lipolysis. Notably, *Cidea*-null mice were lean with enhanced glucose disposal and resistance to high-fat diet–induced obesity and diabetes. Less fat accumulation coupled with enhanced glucose disposal in *Cidea*-null mice is probably due to the higher energy expenditure in BAT. Although their leptin levels were lower, *Cidea*-null mice did not have greater food uptake, indicating that they might be hypersensitive to leptin. A similar phenotype was reported in mice lacking the translational inhibitor 4e-bp1 (ref. 20). *Cidea* may be part of a regulatory feedback pathway involving the central nervous system and WAT.

Similar to Cideb, Cidea is localized to mitochondria and forms a complex with Ucp1. Moreover, coexpression of Cidea and a constitutively active form of Ucp1 (Ucp1Δ3) indicates that Cidea can attenuate the uncoupling activity of Ucp1Δ3 in yeast cells. It is conceivable that one of the biological functions of Cidea *in vivo* is to modulate Ucp1 activity. As Ucp1 is present in great excess in BAT mitochondria, and its *in vivo* uncoupling activity is much below its H^+ transport capacity, Cidea inhibition of Ucp1 activity may finely tune Ucp1 activity and contribute to the 'masking' effect of Ucp1 under physiological conditions[5]. Alternatively, Cidea inhibition of Ucp1 may increase the threshold for Ucp1 activity, rendering thermogenesis more sensitive to Ucp1 concentration in certain critical ranges. Loss of Cidea inhibition would then result in enhanced uncoupling activity and stimulation of lipolysis, leading to greater energy expenditure, rapid depletion of fat storage and a lean phenotype. Although *Ucp1*-null mice were not obese (possibly owing to compensation by other metabolic processes[14,15]), increasing uncoupling activity by overexpressing Ucp1 or Ucp3 in transgenic mice clearly prevented obesity[11,12]. It is also possible that Cidea functions by modulating fatty acid metabolism, as *Cidea*-null mice had much lower concentrations of plasma FFA and triglycerides and lower fatty acid release in BAT. Based on these data, Cidea represents the first protein known in BAT to possibly modulate Ucp1 activity and lipid metabolism and contribute to the development of obesity and diabetes.

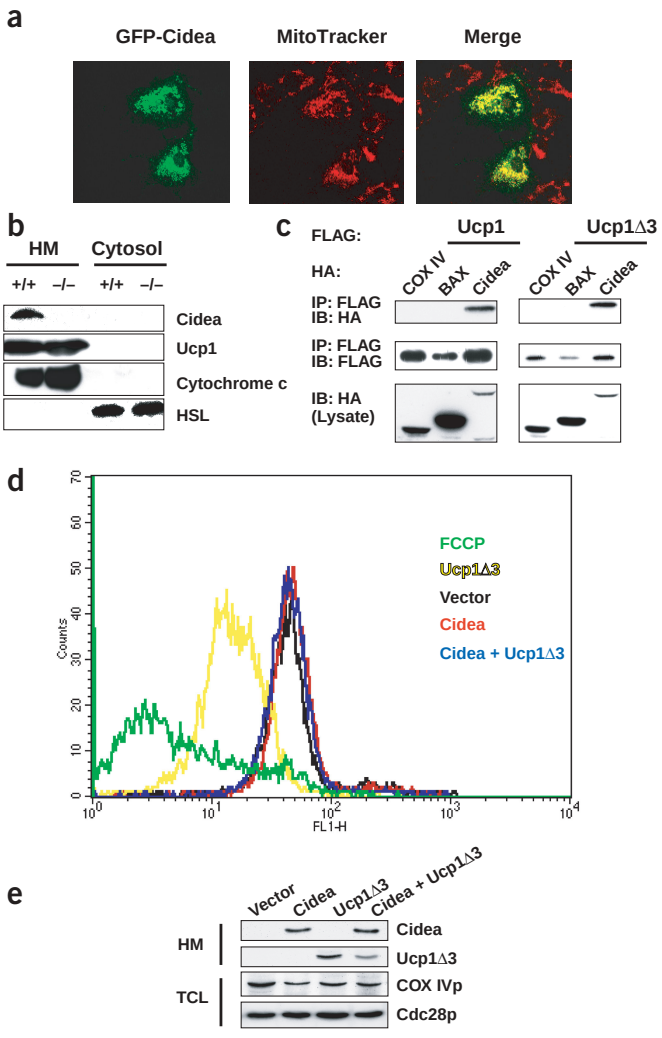

METHODS

Northern-blot, Southern-blot, *in situ* hybridization and RT–PCR analyses. We isolated total RNA from tissues of adult mice using the Qiagen RNA preparation kit and synthesized first-strand cDNA using Expand Reverse Transcriptase (Roche Diagnostic). Primer sequences for RT–PCR are available on request. We isolated genomic DNA from mouse tail and carried out northern-blot and Southern-blot analysis as described[21]. To generate a *Cidea*-specific RNA probe, we subcloned a 600-bp fragment of mouse *Cidea* cDNA into pBluescript II *KS* plasmid (Stratagene). This plasmid was either linearized with *Kpn*I and transcribed with T7 RNA polymerase to generate an antisense probe or linearized with *Not*I and transcribed with SP6 RNA polymerase to generate a sense probe (Roche Diagnostic). We carried out hybridization (Amersham Pharmacia) with sagittal sections of wild-type mouse embryos and then developed slides (Kodak) according to the manufacturer's instructions.

Figure 5 Cidea interacts with Ucp1 and inhibits its uncoupling activity in yeast. (**a**) GFP-Cidea proteins (green) colocalized with MitoTracker (red) in COS-1 cells (40× magnification on a confocal microscope). Frame width = 90 μm. (**b**) Subcellular fractionation of BAT from 4-week-old wild-type (+/+) and *Cidea*-null (–/–) mice. HM, mitochondria-enriched heavy membrane fraction. (**c**) Cidea and Ucp1 interact. IP, immunoprecipitation; IB, immunoblot. Mitochondrial outer membrane protein BAX and inner membrane protein COX IV were used as negative controls. The expression levels of hemagglutinin-tagged proteins are indicated in the lower panel (lysate). (**d**) Mitochondrial membrane potential of *S. cerevisiae* expressing vector alone (black), Ucp1Δ3 (yellow), Cidea (red) or Ucp1Δ3 together with Cidea (blue). The numbers of cells (counts, *y* axis) is represented on a linear scale of 1,024 channels. The *x* axis is a logarithmic scale of fluorescence intensity. FCCP was used as a non-specific uncoupler (green). (**e**) Western-blot analysis for Ucp1Δ3 and Cidea. HM, mitochondria-enriched heavy membrane fraction; TCL, total cell lysate. Yeast COX IVp was used as a control for the amount of mitochondria in each yeast strain. Yeast Cdc28p was used as a loading control.

Preadipocyte isolation and differentiation and *in vitro* lipolysis assay. We isolated preadipocytes essentially as described[22]. For differentiation, we induced preadipocytes reaching 95% confluence in Dulbecco's modified Eagle medium supplemented with 1.7 μM insulin, 1 nM T3, 0.5 mM isobutylmethylxanthine, 0.5 μM dexamethasone, 125 nM indomethacin and 1 nM all-trans-retinoic acid for 4-5 d or until multilocular lipid droplets accumulated in the cells. We carried out the *in vitro* lipolysis assay as previously described[23]. Briefly, mice of 5–6 weeks of age fasted for 4 h and were then decapitated. We excised BAT and WAT from the interscapular region and the gonadal region, respectively. We chopped tissues into 400-μm blocks using a McIlwain tissue chopper (Campden Instruments) and distributed the blocks to 50 mg per 60-mm plate in 1 ml of Dulbecco's modified Eagle low glucose medium containing 2% fatty acid–free bovine serum albumin (Sigma). We incubated tissue slices in the medium with or without 10 μM isoproterenol for 1 h. We collected the medium and stored it at –80 °C for measurement of glycerol and NEFA concentrations.

Generation of *Cidea*-null mice. We isolated *Cidea* genomic clones from a P1 c129/SVJ genomic library (Genome Systems). We prepared a replacement targeting construct in which the *Cidea* sequence between *Eco*RI and *Pst*I, including half of the second exon, was removed and replaced with *neo*^{r}. We linearized the targeting plasmid with *Not*I and electroporated it into RW4 embryonic stem (ES) cells (Genome Systems). We identified targeted clones by Southern-blot analysis using an *Nco*I digestion of ES cell genomic DNA. We used two ES cell lines with disruptions in *Cidea* to generate *Cidea*-deficient mice. Unless otherwise indicated, mice were housed in a temperature-controlled room (23 °C) with a 12-h light/dark cycle and had free access to food and water. We obtained normal chow and high-fat diet from Glenforest.

Electron microscopy, lipid volume density and histological analysis. We prepared mouse BAT sections for transmission electron microscopy as described[24], counterstained the semi-thin sections (0.5 μm) with 0.1% Toluidin-blue in distilled water containing 0.1% Borax and viewed them on a Zeiss Axiovert light microscope to determine the ratio of lipid volume density. We calculated the percentage of lipid volume as described[25]. We fixed gonadal WAT sections from nine-month-old mice in formalin, embedded them in paraffin and transversely sectioned them at 10-μm intervals. We then stained slides with hematoxylin and eosin as previously described[24].

Core body temperature, whole-body oxygen consumption, blood chemistry, glucose and insulin tolerance tests, food intake and HSL activity. The mouse protocol was approved by the animal research committee in the Institute of Molecular and Cell Biology. We measured the core body temperature using a rectal probe attached to a digital thermometer (Yellow Springs Instruments). Mice fasted for 12 h before we placed them in a room at 4 °C for cold-exposure experiments. For blood chemistry, we collected blood by cardiac puncture from fed mice or mice that had fasted for 12 h. We froze serum in aliquots and stored them at –20 °C. We used enzymatic assay kits to determine serum levels of glycerol (Roche Diagnostic) and NEFA (Wako Chemical). We measured levels of serum insulin and leptin using ELISA kit (Research Diagnostic). Serum triglycerides levels were determined by the diagnostic laboratory of National University Hospital of Singapore. We measured glucose levels from tail blood with a hand-held glucose test monitor (Accutrend-GCT, Roche Diagnostic) and disposable test strips.

We carried out glucose and insulin tolerance tests (GTT and ITT, respectively) by intraperitoneal injection of glucose (1.5g per kg body weight) and recombinant human insulin (0.75 unit per kg body weight; Eli Lilly), respectively, into mice. We took tail blood samples before (0 min) and 15, 30, 60, 90 and 120 min after injection to measure glucose levels. Mice fasted for 16 h or 4 h for GTT or ITT, respectively. We assessed whole-body oxygen consumption rates and respiration exchange rates individually in 1-year-old male mice (12 each) fed a standard chow diet using computer-controlled open-circuit indirect calorimetry (Oxymax, Colombus Instruments) with an air flow of 0.6 l min^{-1} and sample flow of 0.5 l min^{-1} at 23 °C. After mice adapted to the metabolic chamber for 8 h, we measured VO_2 at 15-min intervals for 10 h at night. We measured daily food intake by weighing the food given and food remaining every day at 10:00 am in 8-week-old mice for 1 month.

We measured HSL activity as described previously[26]. Briefly, we dissected BAT and WAT from mice after they fasted for 4 h, homogenized it in 3 ml buffer per g tissue and centrifuged it at 110,000*g* for 45 min. We used the fat-depleted infranatant to measure HSL activity using Lipase kit (RDI).

Adiposity index and DNA and lipid contents. We dissected gonadal, mesenteric, retroperitoneal, subcutaneous and inguinal fat pads from F_2 129/C57 wild-type and *Cidea*-null mice according to various anatomical landmarks. We rinsed the fat pads in saline and weighed them on a Mettler AE 50 fine balance. We calculated adiposity index as the total weight of white fat pads from these five locations divided by the total body weight. We determined the DNA and lipid contents by extracting total DNA and lipids from the gonadal fat pad as previously described[26].

Transient transfection, immunoprecipitation, western blotting and mitochondrial localization. We followed detailed protocols for transfection, immunoprecipitation, western-blot analysis and Cidea mitochondrial localization analysis as described[19]. Typically, we used 8 μg of total DNA and 24 μg of DOSPER (Roche Diagnostic) for transfecting each 60-mm plate. For immunoprecipitation, we used 10 μl of Anti-FLAG M2-Agarose Affinity Gel (Sigma). For western-blot analyses, we used rabbit antibody to FLAG (Affinity Bioreagents), antibody to hemagglutinin (Santa Cruz), antibody to Cidea (Chemicon), antibody to Ucp1 (Research Diagnostic), antibody to mouse or yeast COX IV (Molecular Probe), antibody to cytochrome c (Pharmagen), antibody to Actb (Sigma), antibody to HSL (gift from F. Kraemer, Stanford University) and goat secondary antibody to rabbit (Bio-Rad). For mitochondrial localization, we transfected 3 μg of DNA encoding GFP-Cidea into COS-1 cells grown on a 22 × 22–mm cover slip using DOSPER. Twenty-four hours after transfection, we incubated cells with 100 nM MitoTracker-Red (Molecular Probes, USA) for 30 min at 37 °C. We fixed treated cells with 4% paraformaldehyde in phosphate-buffered saline for 20 min and permeabilized them in 0.2% Triton X-100 for 10 min. We visualized cells using Zeiss Axiophot equipped with the Bio-Rad MRC1024 confocal system.

For mitochondria-enriched heavy membrane preparation, we homogenized BAT in MS buffer (210 mM mannitol, 70 mM sucrose, 5 mM Tris-HCl (pH 7.5), 1 mM EDTA and 0.5% bovine serum albumin, with 1 mM phenylmethylsulfonyl fluoride, 5 μg ml^{-1} aprotinin, 1 μg ml^{-1} leupeptin and 1 μg ml^{-1} pepstatin). We centrifuged the homogenate at 700*g* for 10 min to remove unbroken cells and nucleus. We centrifuged the supernatant again at 14,000*g* for 15 min to pellet the heavy membrane fraction. The resultant supernatant is the cytosolic fraction.

Plasmid construction, expression of Ucp1Δ3 and Cidea in yeast and measurement of mitochondrial potential. We amplified *Ucp1* cDNA by PCR, digested it with *Bam*HI and *Xho*I and subcloned it into pXJ40 N-terminal FLAG-tagged vector. Ucp1Δ3 was made by site-directed mutagenesis (Stratagene; ref. 7). We subcloned full-length human *CIDEA* cDNA into pCMV5 as described previously for *CIDEB*[17]. We subcloned Ucp1Δ3 and Cidea into pRS315 and pRS316, respectively, and transformed these into diploid *Saccharomyces cerevisiae* (strain w303) alone or in combination. We grew yeast cells, induced protein expression, prepared yeast mitochondria-enriched heavy membrane and measured mitochondrial membrane potential by a flow cytometer (Beckman-Coulter) as described previously[7]. We used 25 nM of DiOC6 (Molecular Probes) for staining. We added 10 μM of FCCP (Sigma) 10 min before adding DiOC6.

Statistics. All data are presented as mean ± s.e.m. We assessed differences between groups by two-tailed non-paired or paired Student's *t*-test using the Graphpad Prism statistical software.

ACKNOWLEDGMENTS

We thank B. Tang and E. Manser for their critical comments on the manuscript; D. Lai for help in statistical analysis; S. Moochhala for providing the animal metabolic facility; H. Horstmann, L. Hwang, H. Lu, H. Ng, B. Chua, G. Zeng and E. Wong for technical help; and W. Hofmann for his suggestions. This work was supported by Agency for Science, Technology and Research in Singapore.

COMPETING INTERESTS STATEMENT

The authors declare that they have no competing financial interests.

Received 13 March; accepted 14 July 2003
Published online at http://www.nature.com/naturegenetics/

1. Spiegelman, B.M. & Flier, J.S. Obesity and the regulation of energy balance. *Cell* **104**, 531–543 (2001).
2. Lowell, B.B. & Spiegelman, B.M. Towards a molecular understanding of adaptive thermogenesis. *Nature* **404**, 652–660 (2000).
3. Lowell, B.B. & Flier, J.S. Brown adipose tissue, β-3-adrenergic receptors, and obesity. *Annu. Rev. Med.* **48**, 307–316 (1997).
4. Himms-Hagen, J. Brown adipose tissue thermogenesis: interdisciplinary studies. *FASEB J.* **4**, 2890–2898 (1990).
5. Klingenberg, M. & Echtay, K.S. Uncoupling proteins: the issues from a biochemist point of view. *Biochim. Biophys. Acta.* **1504**, 128–143 (2001).
6. Enerback, S. *et al.* Mice lacking mitochondrial uncoupling protein are cold-sensitive but not obese. *Nature* **387**, 90–94 (1997).
7. Bouillaud, F. *et al.* A sequence related to a DNA recognition element is essential for the inhibition by nucleotides of proton transport through the mitochondrial uncoupling protein. *EMBO J.* **13**, 1990–1997 (1994).
8. Echtay, K.S., Winkler, E. & Klingenberg, M. Coenzyme Q is an obligatory cofactor for uncoupling protein function. *Nature* **408**, 609–613 (2000).
9. Dulloo, A.G. & Miller, D.S. Energy balance following sympathetic denervation of brown adipose tissue. *Can. J. Physiol. Pharmacol.* **62**, 235–240 (1984).
10. Lowell, B.B. *et al.* Development of obesity in transgenic mice after genetic ablation of brown adipose tissue. *Nature* **366**, 740–742 (1993).
11. Kopecky, J., Clarke, G., Enerback, S., Spiegelman, B. & Kozak, L.P. Expression of the mitochondrial uncoupling protein gene from the aP2 gene promoter prevents genetic obesity. *J. Clin. Invest.* **96**, 2914–2923 (1995).
12. Clapham, J.C. *et al.* Mice overexpressing human uncoupling protein-3 in skeletal muscle are hyperphagic and lean. *Nature* **406**, 415–418 (2000).
13. Bachman, E.S. *et al.* βAR signaling required for diet-induced thermogenesis and obesity resistance. *Science* **297**, 843–845 (2002).
14. Liu, X. *et al.* Paradoxical resistance to diet-induced obesity in UCP1-deficient mice. *J. Clin. Invest.* **111**, 399–407 (2003).
15. Kozak, L.P., Kozak, U.C. & Clarke, G.T. Abnormal brown and white fat development in transgenic mice overexpressing glycerol 3-phosphate dehydrogenase. *Genes Dev.* **5**, 2256–2264 (1991).
16. Inohara, N., Koseki, T., Chen, S., Wu, X. & Nunez, G. CIDE, a novel family of cell death activators with homology to the 45 kDa subunit of the DNA fragmentation factor. *EMBO J.* **17**, 2526–2533 (1998).
17. Zhou, P., Lugovskoy, A.A., McCarty, J.S., Li, P. & Wagner, G. Solution structure of DFF40 and DFF45 N-terminal domain complex and mutual chaperone activity of DFF40 and DFF45. *Proc. Natl. Acad. Sci. USA* **98**, 6051–6055 (2001).
18. Lugovskoy, A.A. *et al.* Solution structure of the CIDE-N domain of CIDE-B and a model for CIDE-N/CIDE-N interactions in the DNA fragmentation pathway of apoptosis. *Cell* **99**, 747–755 (1999).
19. Chen, Z., Guo, K., Toh, S.Y., Zhou, Z. & Li, P. Mitochondria localization and dimerization are required for CIDE-B to induce apoptosis. *J. Biol. Chem.* **275**, 22619–22622 (2000).
20. Tsukiyama-Kohara, K. *et al.* Adipose tissue reduction in mice lacking the translational inhibitor 4E-BP1. *Nat. Med.* **7**, 1128–1132 (2001).
21. Sambrook, J., Fritsch, E.F. & Maniatis, T. *Molecular Cloning: A Laboratory Manual* (Cold Spring Harbor Laboratory Press, Cold Spring Harbor, New York, 1989).
22. Klein, J. *et al.* β(3)-adrenergic stimulation differentially inhibits insulin signaling and decreases insulin-induced glucose uptake in brown adipocytes. *J. Biol. Chem.* **274**, 34795–34802 (1999).
23. Haemmerle, G. *et al.* Hormone-sensitive lipase deficiency in mice causes diglyceride accumulation in adipose tissue, muscle, and testis. *J. Biol. Chem.* **277**, 4806–4815 (2002).
24. Carson, F.L. *Histotechnology: A Self-Instructional Text* 2nd edn. (American Society for Clinical Pathology Press, Chicago, 1997).
25. Lucocq, J. Unbiased 3-D quantitation of ultrastructure in cell biology. *Trends Cell Biol.* **3**, 354–358 (1993).
26. Martinez-Botas, J. *et al.* Absence of perilipin results in leanness and reverses obesity in *Lepr*$^{db/db}$ mice. *Nat. Genet.* **26**, 474–479 (2000).